

Received July 19, 2018, accepted August 23, 2018, date of publication September 6, 2018, date of current version October 8, 2018.

Digital Object Identifier 10.1109/ACCESS.2018.2869017

# Reliability Study and Thermal Performance of LEDs on Molded Interconnect Devices (MID) and PCB

MAHDI SOLTANI<sup>1</sup>, MORITZ FREYBURGER<sup>1</sup>, ROMIT KULKARNI<sup>2</sup>, RAINER MOHR<sup>1</sup>, TOBIAS GROEZINGER<sup>2</sup>, AND ANDRÉ ZIMMERMANN<sup>1,2</sup>

<sup>1</sup>Institute for Micro Integration, University of Stuttgart, 70569 Stuttgart, Germany

<sup>2</sup>Hahn-Schickard, 70569 Stuttgart, Germany

Corresponding author: Mahdi Soltani (mahdi.soltani@ifm.uni-stuttgart.de)

This work was supported by the Project Configurable LED-lighting with modular design based on 3D-MID (iLED MID) through the German Federal Ministry of Education and Research BMBF under project number 16ES0201.

**ABSTRACT** Light-emitting diodes (LEDs) have increasingly replaced conventional lamps in the fields of general lighting and consumer electronics. In addition to the sharp price fall, this is also due to the significantly higher energy efficiency and the smaller, more compact design. Recently, their robustness and reliability have also reached a level of quality that surpasses the characteristics of conventional light sources such as halogen and fluorescent lamps. Characteristics, such as excellent design freedom and the possibility for functional integration, highlight the main qualities of molded interconnect devices (MIDs). The use of this technology does not only open doors to extend the application field of LEDs to new products but also presents challenges to the lighting industry. There are many studies dealing with the reliability of LEDs as well as with the usability of the MID technology in different fields. But, the lack of experience from the manufacturers regarding the behavior of this interesting configuration (LED/MID) over the entire life cycle prevents this technology from establishing and consolidating its existence. As LEDs in the automotive sector, especially within headlamps, assume increasingly powerful lighting tasks and are no longer used exclusively for signal transfer or for displays, thermal properties of the substrate materials and the thermo-mechanical behavior of the assembly are particularly relevant. In this context, this paper presents a deep and detailed reliability investigation of this system (LED/MID) and examines the influence of the MID substrate choice on the long-term performance of the LED. The impact of the forward current and of the ambient temperature on the junction temperature of the LED is a proven fact. Therefore, the MID effect was inspected under different operating conditions based on infrared thermography. After analyzing the occurred failure mechanisms, by means of X-ray analysis, thermal transient testing and microscopy, the resulting lifetime model is also presented and discussed.

**INDEX TERMS** Light emitting diode, LED, molded interconnect device, MID, PCB, FR4, reliability test setup, thermal management, accelerated lifetime test, reliability, Arrhenius, failure mechanism, lifetime model.

## I. INTRODUCTION

Forecasts from the year 2012 predicted a growth of the LED market of 5% averaged over all areas of lighting technologies [1], which was even exceeded in 2016. Recent market surveys predict that light-emitting diodes will continue to grow at a rate of 7% per year. For the automotive and general lighting sectors, disproportionate growth is expected [2]. Standardized reliability tests of LEDs are already being carried out by the leading manufacturers of optoelectronics.

It is unusual for LEDs to show catastrophic failures (no light). Based on the LED quality and application, the lifetime can vary from 3 months to as high as 50000–70000 h [3]. Usually reliability investigations and lifetime evaluation tests for LEDs refer to the IES LM-80-08 test standard and to the IES TM-21-11 estimation method [4]. Statistical analysis of LED lifetime has also been already published in [5] and [6]. But, as mentioned before, the focus of this work is to investigate the effect of the MID material on the LED.

Thus, the conducted study will be based on the JEDEC and EIAJ standards [7]–[10] to rapidly get results on accelerated degradation. Sometimes, data sheets of LEDs contain the results of such tests under given test conditions. Typically, the test conditions as well as the number of failed LEDs after a predetermined time are mentioned. The benefit for the user is the ability to estimate the lifetime for the intended application. According to the standards [11], [12], the failure criteria are usually based on two performance indicators. First and foremost, an LED is considered to fail if the light intensity falls down a certain percentage of its original value. Common factors are 70, 80 or 90% of the initial value. For a more accurate lifetime model, the 70% criterion is considered in this work.

The second failure criterion is the electrical forward voltage. By an increase to a defined threshold - typically 110 or 120% of the original value - by a constant current supply, the LED counts as failed because the ohmic equivalent resistance of the semiconductor has increased and too much heat is released.

The lifetime tests of the leading LED suppliers typically take place on rigid FR4 printed circuit boards with or without heat-conducting metal core. However, innovative substrate technologies, such as molded interconnect devices (MID), allowing three-dimensional shapes and geometry, also offer the possibility to directly integrate electrical functions into the molded part. This saves production costs by reducing the number of different parts and offers creative design potential that is almost not possible with conventional rigid printed circuit boards.

Fig. 1 illustrates the 3D-MID lighting module developed in the scope of the research project “iLED MID”, where the applied MID technology offers not only the required and aimed 3D design freedom but also the electrical and the



**FIGURE 1.** The 3D-MID lighting module developed in the scope of the research project iLED MID.

mechanical integration of functions in the same circuit carrier. But, at the same time, this technology constitutes a new challenge to the industry, since thermal and thermomechanical aspects of the filled substrate should be given more attention. For the industrial use of this technology, comparable lifetime tests on MIDs are necessary to validate their applicability.

Many studies have been conducted on LED behavior under predefined operating conditions [13]–[15]. Under these different conditions, different failure modes and mechanisms can emerge [16]. The LED reliability is also affected by the packaging; this issue was discussed in [17]. Studies focusing on investigating LED lifetime models in general, by providing different approaches for accelerated life tests, can be found in [18]–[21]. Several research works focused on the thermal performance of LEDs on MIDs [22]–[25], by illustrating different heat dissipation concepts and their effects on the heat generated in the p-n junction. Other works took a deeper look at the reliability of surface mounted devices on MIDs under thermal cycling loading by investigating the thermomechanical behavior and the void formation in the solder joints [26]–[28]. But, as mentioned before, there are currently no detailed investigations about the long-term reliability of LED on MID and, consequently, about their lifetime by taking into account the effect of the substrate material. The long-term behavior of LEDs on MID is still not explored enough.

In what follows, section II gives an overview about the test setup developed to perform the reliability investigations and a description of the test specimen and of the experimental procedure. The full factorial design of experiments with all the factors and their corresponding levels is also presented in this section. The investigation results, the analysis of the occurred failure mechanisms and the resulting lifetime model are illustrated and discussed in section III. Conclusions are presented in section IV.

## II. LED LIFETIME ANALYZER AND EXPERIMENTAL PROCEDURE

### A. TEST SETUP

This section presents the test setup developed during the work and used to investigate the LED reliability. The task has two prerequisites. First, the capability to test a large number of LEDs should be given in order to assure statistic validity; and second the possibility to test under different conditions, particularly at different forward current levels and ambient temperatures (testing in climatic chamber). In addition to measuring the emitted light from LEDs over a long period of time, it is also necessary to detect the voltage at the LED as well as the temperature of its solder joint. In order to solve these subtasks separately, the test setup is separated into several modules. Fig. 2 gives an overview of the complete setup including its submodules.

A computer is needed to set the current levels, configure the layout, and read and save the data. It communicates with the actual test system, which consists of a microcontroller on

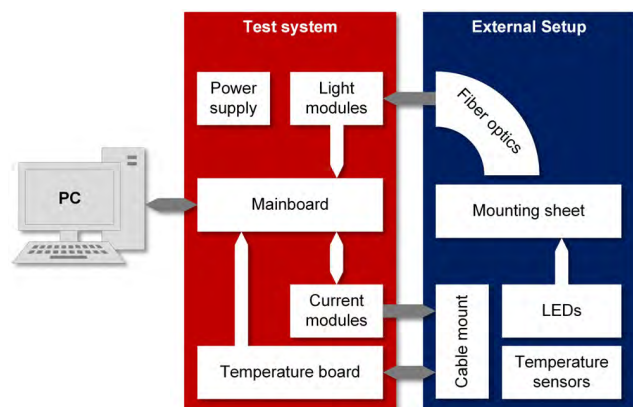


FIGURE 2. Overview of the overall test setup.

a mainboard and the measuring boards. In addition, the in-house developed “LED Lifetime Analyzer” software, which runs on the PC, represents the human-machine interface. Additionally, two power supply units provide the needed energy to carry out the measurement and to operate the LEDs. A cable connection to the external setup supplies the LEDs with current and ensures the voltage and the temperature measurement. Thereby, the external setup is separated from the actual test system in order to protect the measurement boards against temperature and external influences. The emitted light of the driven LEDs is coupled through optical fibers back to the test system, where it is evaluated by the so-called light modules. Fig. 3 gives an overview of the built-up assembly of the complete test system. Up to 8 current modules can be integrated in the test system; each one of them can drive up to 8 LEDs with a predefined current level. This results in a maximum of 64 LEDs that can be powered and controlled simultaneously by the test setup. The current modules also incorporate multiplexers and voltage taps on the terminals of all LED contact pads, allowing the voltage measurement of each LED. Up to 8 light modules, with 8 light sensors each, allow the measurement of the emitted light. The captured illuminance is then guided through fiber optics to reach the light sensors mounted on the light modules. The temperature board allows the measurement of up to 64 temperature values with the help of platinum resistors. For this purpose, a constant current source based on an operational amplifier is installed on the board.

## B. EXPERIMENTAL PROCEDURE

The manufacturing process of MID substrates, based on the laser direct structuring method, includes the steps illustrated in Fig. 4. First, the laser structuring is carried out on the injection molded part, which contains laser-activatable additives. After a cleaning step, the metallization, more precisely the electroless plating process, takes place. If thicker metallization layers are required, an additional electroplating step is conducted. A typically used metallization layer sequence consists of a copper layer (about  $7 \mu\text{m}$ ), responsible for

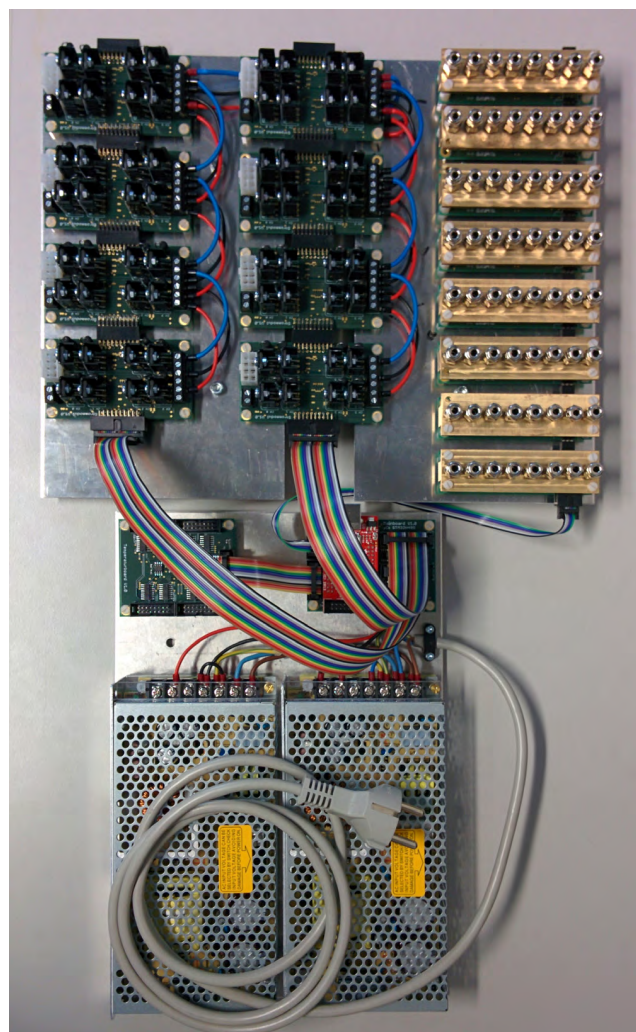


FIGURE 3. Top view of the assembled test system; current modules (top, left), light modules (top, right), temperature board (middle, left), mainboard (middle, right) and the two power supply units (bottom).

the electrical conduction, a nickel layer (about  $7 \mu\text{m}$ ), as a diffusion barrier, and a gold layer, as surface finish (about  $0.1 \mu\text{m}$ ) [26].

For this work, the tested MID substrates are made of “LCP” (Vectra LCP E840i LDS) known for lower coefficient of thermal expansion (suitable for thermo-mechanically critical applications), and “PPA” (TECACOMP®PPA LDS black 4109V) with higher thermal conductivity. Both materials are suitable for the LDS process. As reference material, substrates made of standard printed circuit board (PCB) material (FR4) were also evaluated. These substrates were self-designed with respect to geometric dimensions.

Thermal conductivity of highly filled thermoplastics depends not only on geometry (e.g. substrate thickness) but also on factors such as filler conductivity, filler geometry, filler fraction and injection molding process. Therefore, in-plane (x, y) and through-plane (z) measurements on the

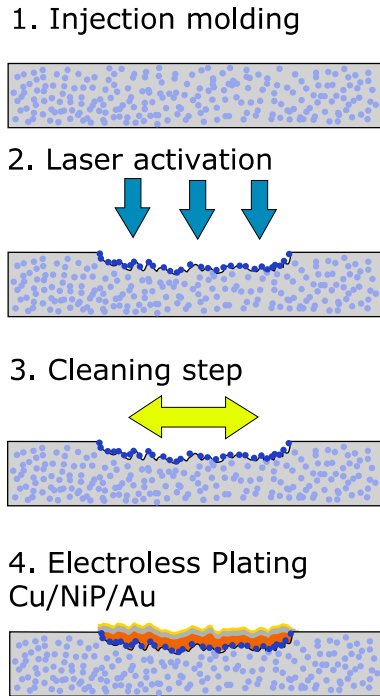


FIGURE 4. The manufacturing process of molded interconnect devices using the laser direct structuring method.

TABLE 1. Substrate thermal characteristics.

SUBSTRATE	MEASURED THERMAL CONDUCTIVITY (W/m·K)		
	<i>x</i>	<i>y</i>	<i>z</i>
<i>LCP</i>	2.4	1.5	0.3
<i>PPA</i>	3.5	3	0.8
<i>FR4</i>	0.8	0.8	0.5

used substrates, by means of the laser flash method (LFA), are necessary. Table 1. reports the measurement results.

Two types of structures are usually used for LEDs. The first one is based on an internal heat sink (especially for high power LEDs). The second approach is to directly mount the chip on the lead frame by using electrically conductive (one bond wire) or non-conductive (two bond wires) die attach. X-Ray measurements, cross sections and microscopy pictures show that the low power LED, chosen for this study, has the second structure (see Fig. 5). In fact, the chip of this LED is mounted on the lead frame, by means of thermally conductive die attach. This adhesive is only responsible for the thermal dissipation, and the electrical current is conducted through two bond wires connected to the leads. One of these leads (anode side), on which the chip is mounted, is the thermally active lead. The other lead (cathode side) is relevant only for the electrical conductivity. This LED features a dominant wavelength equal to 470 nm (blue), has a viewing angle of 120° and a maximum forward current of 25 mA. Typical

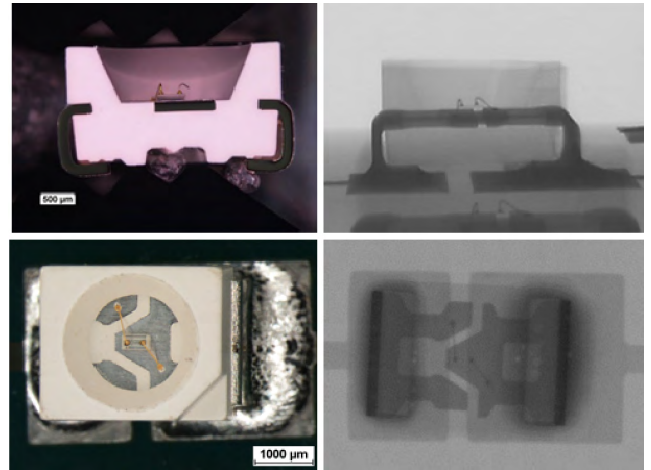


FIGURE 5. X-Ray measurements (right), cross sections (top, left) and microscopy pictures (left) show the structure of the used LED.

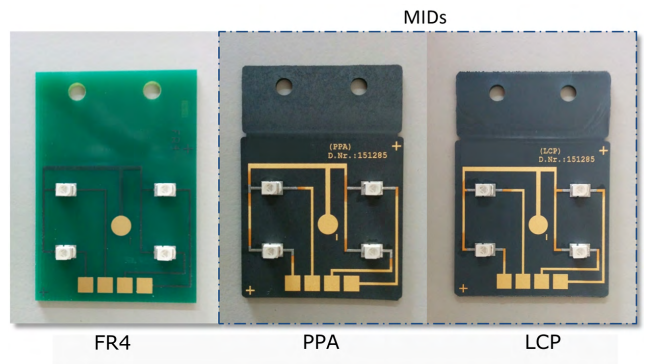


FIGURE 6. Examples of the used test specimen equipped with LEDs. Left: Standard FR4 PCB. Right: Two MIDs based on PPA and LCP materials.

forward voltage value is 3.2 V across a current of 20 mA (64 mW electrical power). Of course, the developed system can operate with any other kind of LED having similar characteristics. Examples for the used self-designed test specimen with mounted LEDs are shown in Fig. 6.

The impact of the forward current and the ambient temperature on the junction temperature of the LED is a well-known and proven fact [3]. Higher current levels implicate higher levels of heat dissipated at the junction. This applies to the ambient temperature, too. Note that this junction temperature should be kept as low as possible, otherwise undesirable effects can emerge. These can include less reliability, shorter lifetime and even color shift in the LED [3]. In order to address these effects, two ambient temperature levels (85°C and 105°C) were chosen following the DIN standards [11], [12] and further tests were conducted at 25°C to validate the lifetime model. Two forward current levels (75mA and 100 mA) have been chosen after many experimental trials under different test conditions, in order to avoid overstressing, and consequently, to address the same failure mechanism. This experimental study was planned using the statistics software Minitab. Table 2. illustrates the full factorial design of

**TABLE 2. Full factorial design of experiments (DoE) relevant factors and their corresponding levels.**

FACTORS	CORRESPONDING LEVELS		
Forward current	75 mA	100 mA	
Ambient Temperature	25°C	85°C	105°C
Material	LCP	PPA	FR4

experiments and shows the relevant factors and their corresponding levels. Due to the fact that the temperature levels were maintained constant over the test duration, the effect due to thermal resistance was given more attention in this work than the effect due to the mismatch in the thermal expansion coefficient.

In this context, it is worthwhile noticing that the temperature in the climatic chamber, which was measured during pre-tests by temperature sensors spread across the oven, was evenly distributed (see Fig. 7). So, it can be assumed that, the LEDs are tested under the same conditions. Fig. 8 presents the arrangement of the used substrates in the chamber. Fig. 9 shows the external setup in the climatic chamber with test substrates and fiber optics spread across the mounting plate. Note that the fiber optics and all the cables used were chosen in accordance to their thermal stability. The illuminance values of the tested LEDs were measured simultaneously. To avoid any possible interference, many pre-tests were conducted to optimize the geometry boundaries (space between LEDs, distance between LED and fiber etc.) by considering the viewing angle of the tested LED. In order to create the aimed lifetime model, junction temperature should be measured. Conventional methods such as Pt100 sensors or even thermography are not sufficiently accurate to directly measure the chip temperature. In order to address this issue, both thermal transient and thermographic tests were carried out. An infrared camera was used to measure the solder temperature on the thermally active side. An important parameter for this kind of measurement is emissivity. The emissivity  $\epsilon$  depends not only on the surface color but also on its finish [29]. To take this effect into consideration, a comparative calibration approach thanks to a black coating, which has a homogeneous emissivity of about 0.97, was conducted. Emissivity values of about 0.96 for LCP and PPA, 0.98 for FR4, 0.89 for the LED and 0.35 for the solder surface were measured. In Fig. 10, an example of a thermal image taken by the thermal camera is portrayed for visualization. The pitch between two neighboring LEDs was adapted to minimize mutual interactions.

In order to get the correct temperature at the junction, transient thermal measurements have to be carried out. With the help of a T3Ster® equipment from Mentor Graphics, the thermal behavior of the investigated system and the

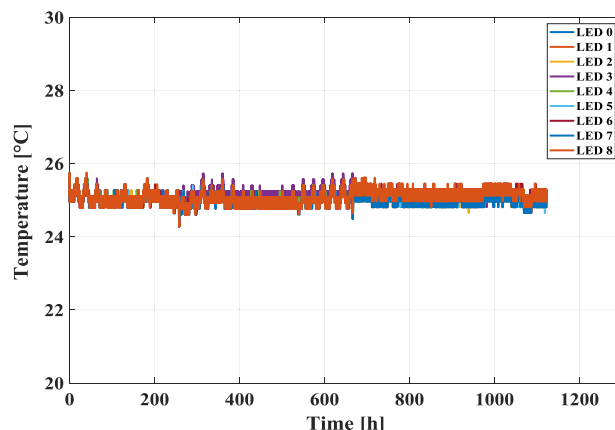


**FIGURE 7. Variation of the temperature of the substrate surface over time of a sample of 9 LEDs spread across the climatic chamber.**

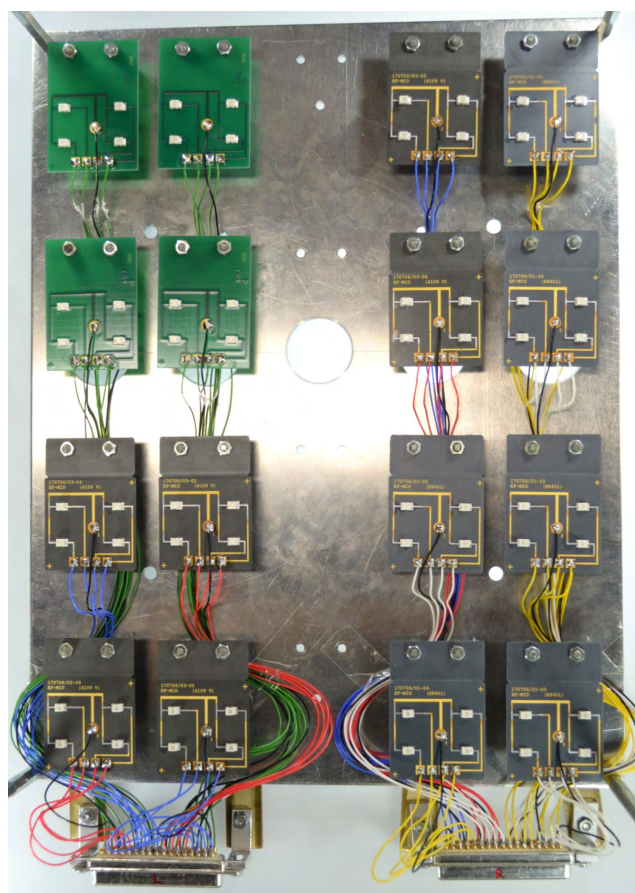


**FIGURE 8. Arrangement of different substrates in the climatic chamber.**

contribution of each existing part and interface to the overall thermal resistance can be captured. This measurement method is conducted conform to the guidelines given in the JEDEC standard JESD51-1, where the way to derive the thermal resistance of LED systems is described. This equipment is used to record, in this case, the cooling curve and to deduce the R-C network and the structure functions from it [30]–[34].

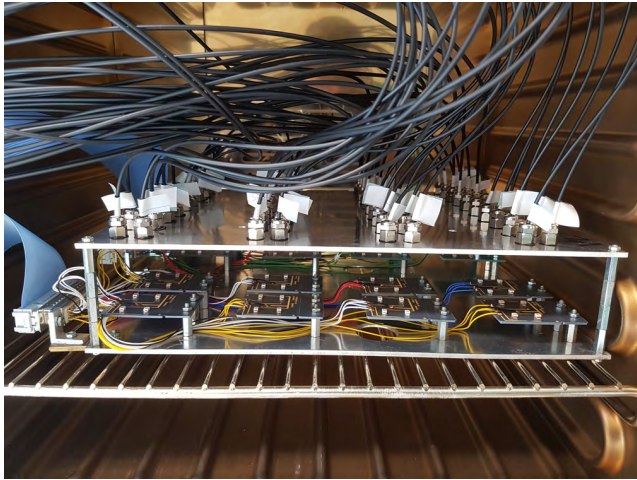


FIGURE 9. The external setup in the climatic chamber.

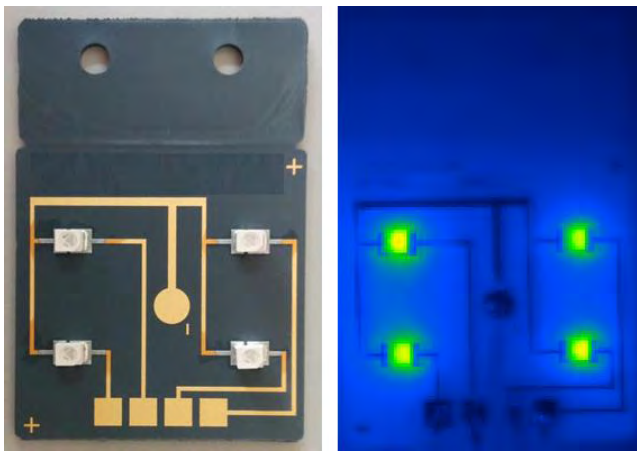


FIGURE 10. Left: Example of a test specimen equipped with LEDs. Right: Thermal image of the test specimen.

But first of all, the K factor should be determined. This factor defines the relationship between the junction temperature change and the temperature sensitive parameter (TSP). For a diode-like structure, the forward voltage  $V_f$  is typically the most often used parameter for temperature sensing. Therefore, temperature-voltage calibration should be conducted, which means voltage values should be measured at different temperature levels. Fig. 11 shows the results of a K factor calibration, which was conducted based on the following equation

$$K_{factor} = \Delta V_f / \Delta T \quad [\text{mV}/^\circ\text{C}] \quad (1)$$

All measured K factors are around 1.9 mV/°C, which convenes very good with typical values for blue LEDs [35]. In order to obtain accurate measurements by having repeating boundary conditions, a thermostat was used to control the cold plate temperature. First, the samples were driven with 50 mA heating current until reaching thermal steady state conditions. Then, the cooling curve was recorded in the

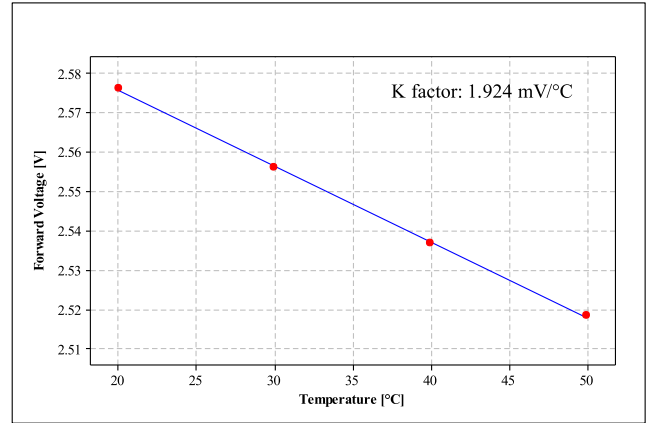


FIGURE 11. The relationship between forward voltage and temperature for the K factor calibration.

temperature range of 20°C to 50°C at a sensing current level of 0.5 mA.

It is fundamentally important to underline the fact, that in order to correctly calculate the thermal resistance, an optical correction should be conducted. That means, only dissipated heat power should be taken into account by reconstructing the thermal path. Consequently, the thermal load has to be derived by subtracting the optical power from the electrical input power. In this study, the optical power was determined using an integrating sphere of a spectrometer. Based on mathematical transformations [36], the structure functions can be determined and the thermal resistance is defined as:

$$R_{th_{j-s}} = (T_j - T_s) / (P_e - P_{op}) = (T_j - T_s) / P_h \quad [\text{K}/\text{W}] \quad (2)$$

where,  $R_{th_{j-s}}$  is the thermal resistance between junction and solder,  $T_j$  is the junction temperature at the chip,  $T_s$  is the solder temperature,  $P_e$  is the electrical power,  $P_{op}$  is the optical power and  $P_h$  is the dissipated heat power. According to (2) and after measuring the solder temperature and the thermal resistance  $R_{th_{j-s}}$ , the junction temperature can be determined via the following equation:

$$T_j = (R_{th_{j-s}} \times P_h) + T_s \quad [\text{K}] \quad (3)$$

### III. RESULTS AND DISCUSSIONS

In this study, 320 LEDs were tested under different operating conditions. Fig. 12 reports as an example the relative illuminance vs. time plot for 2 LEDs from each constellation on PPA. It is noted that, after an initial stage where the illuminances drop down in a faster manner, the aging process downshifts and reaches a plateau. The test was conducted until all LEDs had reached the failure criterion  $L_{70}$ . In the case of LEDs on PPA tested at 25°C / 75 mA, no failure could be detected even after a test duration of more than 5000 h (almost 7 months). During all conducted tests, the case of the voltage exceeding the barrier of 110% did not occur. Works dealing with the analysis of these failure mechanisms, by means of X-Ray analysis, thermal transient testing and microscopy, were conducted. The taken microscopic images

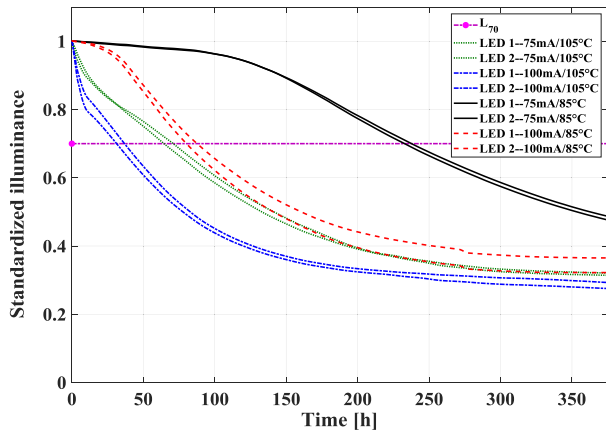


**FIGURE 12.** Example of variation of the illuminance over time of a sample of 2 LEDs for each constellation on PPA.

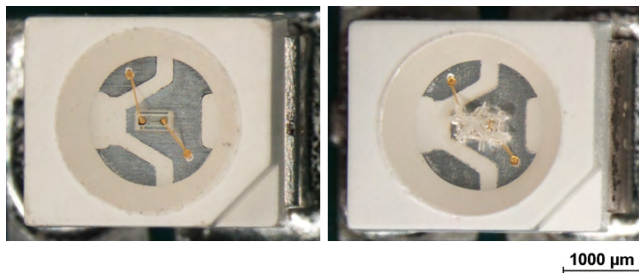


**FIGURE 13.** Left: Example of a new LED. Right: lens cracking at an LED mounted on an FR4 substrate (105°C / 100 mA).

show a first failure mode consisting of lens cracking as shown in the example of LED mounted on an FR4 substrate illustrated in Fig. 13. According to [3], lens cracking is a typical LED failure mechanism, which takes place due to thermomechanical stress caused by high ambient temperature and/or poor thermal design. This engenders lumen degradation of the LED. It was observed that, this effect occurred at the ambient temperature of 105°C (higher ambient temperature), but particularly on LEDs mounted on FR4 substrates (poorer thermal design than the tested MID substrates).

Transient thermal measurements, conducted as described in section II, were also used to identify partial thermal resistances of the different parts, which consist of the thermal path of the investigated system (package + substrate). The resulting cumulative structure functions in Fig. 14 help to determine values of the thermal resistance of each and every one of these parts. In this graph, the change of the slope of the different curve sections indicates that the heat flows from one section (material and/or volume) to another one. A comparison between two new LEDs mounted on different substrates (PPA and LCP) helps to better identify the different sections. Based on the comparison between new and stressed LEDs on same substrates, it can be observed that a significant increase in the thermal resistance of the electrically non-conductive die attach took place. This section is located between the chip and the lead frame. This is also a typical failure mode for

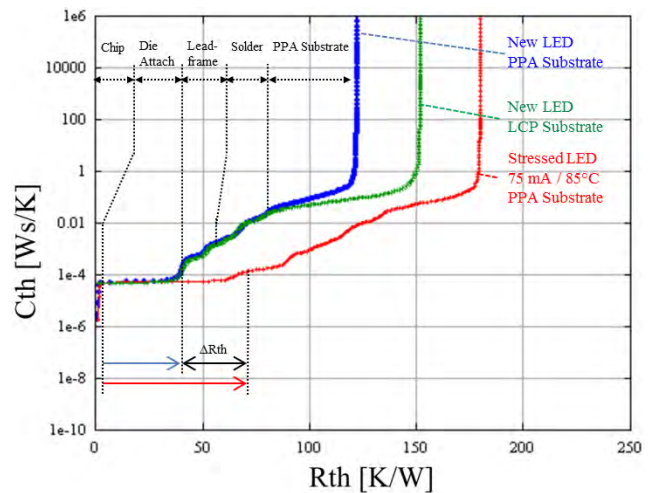


**FIGURE 14.** Cumulative structure function for the new LEDs mounted on PPA and LCP and for a stressed LED at 75 mA / 85°C mounted on PPA.

LEDs [3], [32], which occurs due to mismatch in material properties, especially the coefficient of thermal expansion (CTE). This mismatch leads to thermomechanical stress and also causes lumen degradation.

Other typical failure mechanisms, which can lead to lumen degradation, such as die cracking, or open circuit (no light), such as bond wire fracture or fatigue, can be excluded based on taken X-Ray and microscopy images and due to the fact that, all tested LEDs emitted light during the entire test duration. Table 3. summarizes the occurred failure mechanisms.

Note that, no failure analysis could be done for tests conducted at 25°C. This is because of the fact that, none of the LEDs mounted on PPA and tested at 25°C / 75 mA failed until now. Therefore, this room temperature test cannot be concluded. However, the available results from this 25°C test were also evaluated in order to confirm the lifetime model deduced from the other configurations.

After the evaluation of the gained results, the decision was taken to only consider the most frequently occurring failure, which is the delamination of the die attach, for further investigations.

Utilizing the filtered results, a distribution test was conducted. The evaluated results in the example of PPA, shown in Fig. 15, indicate that the three-parameter Weibull distribution provides the best correlation factors in all cases, which is almost valid for all the other constellations. This can be already seen on the bent curve in the probability network of the Weibull distribution with 2 parameters. This indicates the existence of a failure-free time [37].

For the exponential distribution no correlation coefficients could be calculated, which indicates that no plausible relationship is given between the lifetime data and this distribution function. Fig. 16 contains, as an example, the Weibull plots for the different constellations on PPA, including statistical lifetime parameters and 95% lower and upper confidence

**TABLE 3.** Occurred failures depending on the substrate material and the operating condition.

PPA			
	Initial count	Delamination	Lens cracking
25°C / 75 mA	8	N/A	N/A
25°C / 100 mA	12	N/A	N/A
85°C / 75 mA	24	24	0
85°C / 100 mA	24	24	0
105°C / 75 mA	24	24	0
105°C / 100 mA	24	22	2
LCP			
	Initial count	Delamination	Lens cracking
25°C / 75 mA	12	N/A	N/A
25°C / 100 mA	12	N/A	N/A
85°C / 75 mA	24	24	0
85°C / 100 mA	24	23	1
105°C / 75 mA	20	20	0
105°C / 100 mA	24	21	3
FR4			
	Initial count	Delamination	Lens cracking
25°C / 75 mA	12	N/A	N/A
25°C / 100 mA	8	N/A	N/A
85°C / 75 mA	16	16	0
85°C / 100 mA	16	10	6
105°C / 75 mA	20	20	0
105°C / 100 mA	16	10	6

\*N/A: Not applicable

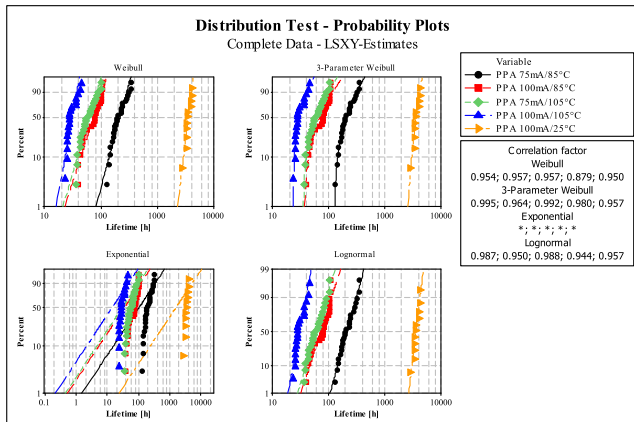


**FIGURE 15.** Distribution test with correlation factors for all tested constellations on PPA: Weibull, 3-Parameter Weibull, Exponential and Normal distributions.

intervals. The shape factor of more than one indicates aging behavior.

The characteristic lifetime  $LT$  was determined at 63.2%, according to [38]. It is the time at which 63.2% of the LEDs failed. In Fig. 17, the main effects plots (averaging mean values) for the initial junction temperature and for the characteristic lifetime, depending on the material of the

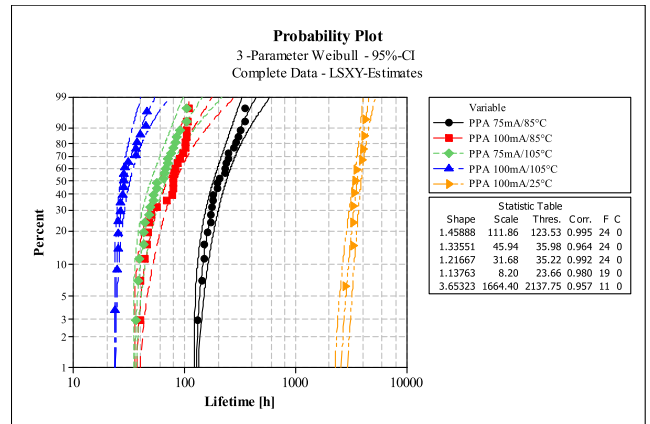


**FIGURE 16.** Probability plot on the basis of 3-Parameter Weibull distribution, including 95% lower and upper confidence interval (PPA as an example).

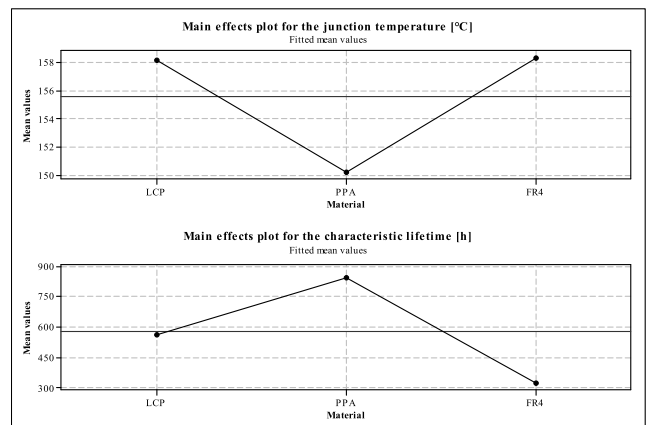


**FIGURE 17.** Main effects plots for the initial junction temperature and for the characteristic lifetime depending on the material of the used substrate.

used substrate, are shown. According to these main effects plots, it is clearly perceptible that the material choice has almost the same but opposite leverages on the initial junction temperature  $T_j$  and on the characteristic lifetime  $LT$ . For this reason, it can be concluded that both outcomes correlate with each other. LEDs mounted on substrates with better thermal performance (e.g. PPA) show lower initial junction temperatures and, consequently, have longer lifetime. Fig. 18 presents the characteristic lifetime  $LT$  for the different configurations investigated in this study.

In order to develop lifetime models, two approaches were pursued in this work and a comparison was conducted. The first one consists of developing a generalized model “GM” describing all configurations, with no consideration of direct dependency on any of the investigated factors (Fig. 19). This approach confirms the assumption supported in Fig. 17. The second approach is based on a material dependent model “MM” by taking into account the effect of the choice of the substrate material on the lifetime of the

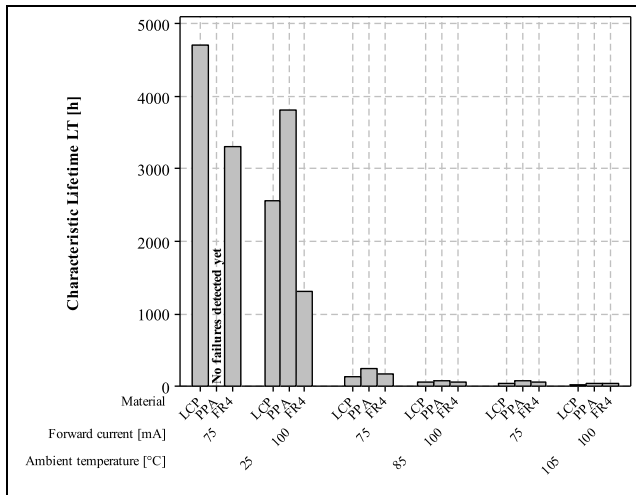


FIGURE 18. Characteristic lifetime *LT* depending on the applied configuration.

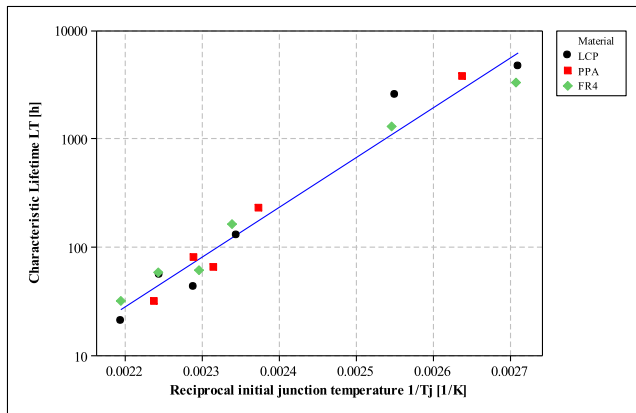


FIGURE 19. Proposed lifetime model, by taking into consideration all investigated configurations (generalized model *GM*).

tested LEDs (Fig. 20). It is common to use an Arrhenius-type equation to estimate the lifetime of a component subjected to thermal effects [39]. All obtained lifetime models, presented in Fig. 19 and 20, seem to obey this rule, since all the determination coefficients  $R^2$  are higher than 0.960. This highlights the excellent fitting quality.

Therefore, the characteristic lifetime *LT* fits the following expression

$$LT = C_T \cdot e^{E_A/k \cdot T_j} \quad [h] \quad (4)$$

where,  $C_T$  is the thermal factor,  $E_A$  is the activation energy,  $k = 8.617385 \cdot 10^{-5} \text{ eV} \cdot \text{K}^{-1}$  is the Boltzmann constant and  $T_j$  is the initial junction temperature in Kelvin. The obtained coefficients and activation energy are summarized in table 4. All the proposed lifetime models, based on both approaches, provide very good fitting parameters and can be used to predict LED lifetime in a very accurate and precise manner. As discussed before, the considered failure mechanism occurs in the LED and not in direct contact with

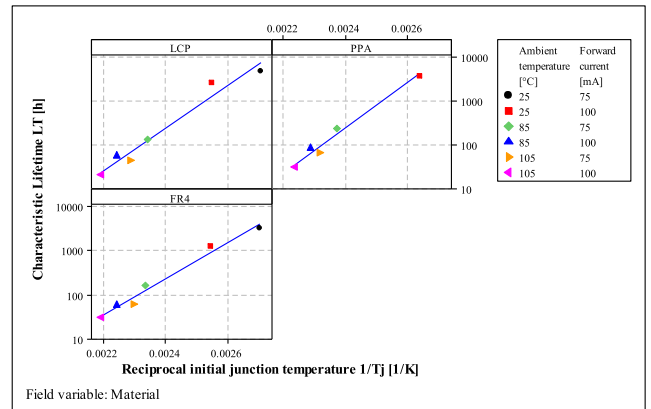


FIGURE 20. Proposed lifetime models depending on the material of the used substrate (Material dependent model *MM*).

TABLE 4. Coefficients and parameters of the obtained generalized lifetime model *GM* and the three material dependent lifetime models *MM*.

Arrhenius Parameters			
Model	$C_T$	$E_A$ [eV]	$R^2$
<i>GM</i>	$2 \cdot 10^{-9}$	0.91	0.963
<i>MM-PPA</i>	$1 \cdot 10^{-10}$	1.01	0.984
<i>MM-LCP</i>	$7 \cdot 10^{-10}$	0.96	0.960
<i>MM-FR4</i>	$4 \cdot 10^{-8}$	0.81	0.979

the substrate. Therefore, and taking into account the high determination coefficient of the generalized model “GM”, it can be assumed that this model can be used to precisely predict the LED lifetime. The effect of the substrate material on the characteristic lifetime is already taken into account through the engendered junction temperature.

Substituting the initial junction temperature of about 65°C generated under normal conditions (at 25 mA and 25°C) in the model delivers an estimated lifetime of about 71322 h (about 8.14 years), which is realistic and convenes with typical data for LED lifetime [3].

#### IV. CONCLUSIONS

The role of molded interconnect devices (MID) in several applications, such as consumer electronics and automotive, has significantly increased recently. Due to the excellent design freedom, MID are becoming more and more attractive for the lighting technologies. As a matter of fact, it must be remembered that thermal issues impact not only the efficiency but also the reliability and the color stability of LED-based systems.

In this context, this work presented a deep and detailed reliability investigation of this system. The influence of the MID substrate choice on the long-term performance of the LED was considered and discussed. Main influencing factors, such as the forward current and the ambient temperature, and their effect on the junction temperature of the LED were

examined closely. Therefore, a full factorial design of experiments was generated and accelerated lifetime tests were conducted under different combined stress conditions. Based on infrared thermography and after analyzing the occurred failure mechanisms, by means of X-ray analysis, thermal transient testing and microscopy, the relationship between the engendered initial junction temperature and the characteristic lifetime was observed and analyzed.

It has been established that the proposed lifetime models, reporting the relationship between characteristic lifetime and initial junction temperature, suit very well with the Arrhenius equation. Two different approaches, a generalized one and a material dependent one, were compared. Both models showed very good accuracy with high determination coefficients. High determination coefficients  $R^2$  of more than 0.960 highlight the excellent fitting quality.

## V. ACKNOWLEDGMENT

The authors would like to thank the different project partners and funding institutes.

## REFERENCES

- [1] *Lighting the Way: Perspectives on the Global Lighting Market*, Vis. Media Eur., McKinsey & Company Inc., New York, NY, USA, 2012, p. 59.
- [2] P. Smallwood, "Lighting, LEDs and smart lighting market overview," presented at the U.S. Dept. Energy SSL Workshop, Raleigh, NC, USA, 2016.
- [3] M.-H. Chang, D. Das, P. V. Varde, and M. Pecht, "Light emitting diodes reliability review," *Microelectron. Rel.*, vol. 52, no. 5, pp. 762–782, May 2012.
- [4] W. D. van Driel, M. Schuld, B. Jacobs, F. Commissaris, J. van der Eyden, and B. Hamon, "Lumen maintenance predictions for LED packages using LM80 data," in *Proc. 16th Int. Conf. Thermal, Mech. Multi-Phys. Simulation Exp. Microelectron. Microsyst.*, 2015, pp. 1–5.
- [5] S. T. Tseng and C. Y. Peng, "Stochastic diffusion modeling of degradation data," *J. Data Sci.*, vol. 5, no. 3, pp. 315–333, 2007.
- [6] J. Fan, K.-C. Yung, and M. Pecht, "Lifetime estimation of high-power white LED using degradation-data-driven method," *IEEE Trans. Device Mater. Rel.*, vol. 12, no. 2, pp. 470–477, Jun. 2012.
- [7] *Temperature, Bias, and Operating Life*, Standard JESD22-A108E, JEDEC Solid State Technology Association, Nov. 2010.
- [8] *Method for Developing Acceleration Models for Electronic Component Failure Mechanisms*, Standard JESD91A, JEDEC Solid State Technology Association, Jan. 2011.
- [9] *Environmental and Endurance Test Methods for Semiconductor Devices*, Standard EIAJ ED-4701/100, Standard of Japan Electronics and Information Technology Industries Association, 2001.
- [10] *Steady-State Temperature-Humidity Bias Life TeST*, Standard JESD22-A101D, JEDEC, 2015. Accessed: Jul. 1, 2018. [Online]. Available: <https://www.jedec.org/standards-documents/docs/jesd-22-a101c>
- [11] *Non-Ballasted LED Lamps—Performance Requirements (IEC 34A/1601/CD:2012)*, Standard DIN EN 62663-2, 2012. Accessed: Jul. 1, 2018. [Online]. Available: <https://standards.globalspec.com/std/1571231/din-en-62663-2>
- [12] *LED Modules for General Lighting—Performance requirements*, Standard IEC 62717:2014+AMD1:2015 CSV, 2015.
- [13] H. C. Chen et al., "Improvement of lumen efficiency in white light-emitting diodes with air-gap embedded package," *Microelectron. Rel.*, vol. 52, no. 5, pp. 933–936, May 2012.
- [14] M. Cai et al., "A reliability analysis method for LED luminaires based on step stress accelerated degradation test," in *Proc. Electron. Packag. Technol. (ICEPT)*, Dalian, China, 2013, pp. 1207–1211.
- [15] H. Huang, M. Cai, K. Tian, Y. Chen, H. Jia, and D. Yang, "Thermal resistance analysis of high power LED module under power cycling test," in *Proc. 15th Int. Conf. Electron. Packag. Technol.*, Chengdu, China, 2014, pp. 1446–1449.
- [16] G. Lu, S. Yang, and Y. Huang, "Analysis on failure modes and mechanisms of LED," in *Proc. 8th Int. Conf. Rel., Maintainability Saf.*, Jul. 2009, pp. 1237–1241.
- [17] L. Guoguang, H. Yun, E. Yunfei, Y. Shaohua, and L. Zhifeng, "The relationship between LED package and reliability," in *Proc. 16th IEEE Int. Symp. Phys. Failure Anal. Integr. Circuits*, Jul. 2009, pp. 323–326.
- [18] A. Albertini, M. G. Masi, G. Mazzanti, L. Peretto, and R. Tinarelli, "A test set for LEDs life model estimation," in *Proc. IEEE Instrum. Meas. Technol. Conf.*, May 2010, pp. 426–431.
- [19] A. Albertini, M. G. Masi, G. Mazzanti, L. Peretto, and R. Tinarelli, "Experimental analysis of LEDs' reliability under combined stress conditions," in *Proc. IEEE Int. Instrum. Meas. Technol. Conf.*, Binjiang, China, May 2011, pp. 1–5.
- [20] A. Albertini, G. Mazzanti, L. Peretto, and R. Tinarelli, "Development of a life model for light emitting diodes stressed by forward current," *IEEE Trans. Rel.*, vol. 63, no. 2, pp. 523–533, Jun. 2014.
- [21] E. Nogueira, V. Orlando, J. Ochoa, A. Fernandez, and M. Vazquez, "Accelerated life test of high luminosity blue LEDs," *Microelectron. Rel.*, vol. 64, pp. 631–634, Sep. 2016.
- [22] M. Barth, R. Kulkarni, M. Soltani, W. Eberhardt, T. Meißner, and A. Zimmermann, "Heat dissipation for MID applications in lighting technology," in *Proc. MID Congr.*, 2016, pp. 1–4.
- [23] T. Leneke and B. Schmidt, *Entwärmungskonzepte Durch Funktionale Strukturen in Spritzgegossenen Dreidimensionalen Schaltungsträgern*. Aachen, Germany: Shaker Verlag, 2013.
- [24] C. Heinle, "Simulationsgestützte Entwicklung von Bauteilen aus wärmeleitenden Kunststoffen," Ph.D. dissertation, Inst. Polymer Technol., Univ. Erlangen-Nürnberg, Erlangen, Germany, 2012.
- [25] M. Soltani, R. Kulkarni, Y. Liu, M. Barth, T. Grözinger, and A. Zimmermann, "Experimental and computational study of array effects on LED thermal management on molded interconnect devices MID," in *Proc. MID Congr.*, Würzburg, Germany, 2018, p. 6.
- [26] T. Grözinger, "Untersuchungen zu Zuverlässigkeit und Lebensdauermodellen für gelötete SMD auf spritzgegossenen Schaltungsträgern," Ph.D. dissertation, Inst. Micro Integr., Univ. Stuttgart, Stuttgart, Germany, 2015.
- [27] P. Wild, T. Grözinger, D. Lorenz, and A. Zimmermann, "Void Formation and Their Effect on Reliability of Lead-Free Solder Joints on MID and PCB Substrates," *IEEE Trans. Rel.*, vol. 66, no. 4, pp. 1229–1237, Dec. 2017.
- [28] P. Wild, D. Lorenz, T. Grözinger, and A. Zimmermann, "Effect of voids on thermo-mechanical reliability of chip resistor solder joints: Experiment, modelling and simulation," *Microelectron. Rel.*, vol. 85, pp. 163–175, Jun. 2018.
- [29] P. Svasta, D. Simion-Zanescu, and R. Ionescu, "Components' emissivity in reflow soldering process," in *Proc. 54th Electron. Compon. Technol. Conf.*, vol. 2, 2004, pp. 1921–1924.
- [30] P. Szabo, A. Poppe, G. Farkas, V. Szekely, B. Courtois, and M. Rencz, "Thermal characterization and compact modeling of stacked die packages," in *Proc. 10th Intersociety Conf. Phenomena Electron. Syst. (ITHERM)*, San Diego, CA, USA, 2006, pp. 251–257.
- [31] A. Poppe et al., "Thermal measurement and modeling of multi-die packages," *IEEE Trans. Compon. Packag. Technol.*, vol. 32, no. 2, pp. 484–492, Jun. 2009.
- [32] J. Hu, L. Yang, and M. W. Shin, "Mechanism and thermal effect of delamination in light-emitting diode packages," *Microelectron. J.*, vol. 38, no. 2, pp. 157–163, Feb. 2007.
- [33] J. H. Choi and M. W. Shin, "Thermal investigation of LED lighting module," *Microelectron. Rel.*, vol. 52, no. 5, pp. 830–835, May 2012.
- [34] A. Gasse et al., "Thermal management: A key point for the integration in solid state lighting systems," in *Proc. Electron. Syst.-Integr. Technol. Conf. (ESTC)*, Helsinki, Finland, 2014, pp. 1–7.
- [35] T. Q. Khanh, P. Bodrogi, Q. T. Vinh, and H. Winkler, Eds., *LED Lighting: Technology and Perception*. Weinheim, Germany: Wiley, 2015.
- [36] G. Farkas and A. Poppe, "Thermal testing of LEDs," in *Thermal Management for LED Applications*, vol. 2. New York, NY, USA: Springer, 2014.
- [37] B. Bertsche and G. Lechner, *Zuverlässigkeit im Fahrzeug- und Maschinenbau: Ermittlung von Bauteil- und System-Zuverlässigkeiten*. Berlin, Germany: Springer, 2004.
- [38] B. Bertsche, P. Göhner, U. Jensen, W. Schinköthe, and H.-J. Wunderlich, *Zuverlässigkeit mechatronischer Systeme: Grundlagen und Bewertung in frühen Entwicklungsphasen*. Berlin, Germany: Springer, 2009.

- [39] A. L. Hartzell, M. G. da Silva, and H. R. Shea, "Lifetime prediction," in *MEMS Reliability*. Boston, MA, USA: Springer, 2011, pp. 9–42.



technology, reliability investigation, and electronics packaging and molding technology (molded interconnect devices).

**MORITZ FREYBURGER** received the B.Sc. and M.Sc. degrees in mechanical engineering from the University of Stuttgart, Germany. In 2017, he accomplished his study research thesis with the Institute for Micro Integration.

**ROMIT KULKARNI** received the bachelor's degree in India, and the master's degree in computational mechanics from the University of Stuttgart, Germany, in 2010. He has two years of experience in the field of project management. Before joining Hahn-Schickard, he has three and half years of experience as a stress calculations engineer in aerospace technology. Since 2014, he has been a Research Associate at Hahn-Schickard with the Modeling, Reliability & Analysis Group. His main areas of activity include injection molding simulations along with its integration into structural mechanics of micro systems.

**RAINER MOHR** received the degree in electrical engineering from the University of Stuttgart in 1979. As part of his studies, he joined the Institute for Watch Technology and Precision Mechanics. The radio clock, a technical challenge then and now, was for a long time his field of work. He is currently responsible for research and teaching at the Institute for Micro Integration in the field of micro-technology.

**TOBIAS GROEZINGER** received the Dipl.Ing. degree in mechatronics and the Dr.Ing. degree in mechanical engineering from the University of Stuttgart, Germany, in 2009 and 2015, respectively. From 2009 to 2015, he was a Research Assistant with the Institute for Micro Integration, Stuttgart. Since 2015, he has been with the Institute for Micro Assembly Technology, Hahn-Schickard, Stuttgart. Since 2016, he has been a Leader with the Modeling, Reliability & Analysis Group.



**ANDRÉ ZIMMERMANN** received the Dipl.Ing. degree in material science with specialization in mechanical engineering and the Ph.D. degree from Technische Universität Darmstadt, Darmstadt, Germany, in 1999. He was with NIST, Gaithersburg, MD, USA, and also with the University of Washington, Seattle, WA, USA. He was a Group Manager with the Max-Planck-Institute for Metals Research, Stuttgart, Germany. He was a Senior Manager of electronic packaging within corporate research and development at Robert Bosch GmbH, Waiblingen, Germany. Since 2015, he has been a Professor in micro technology with the Institute for Micro Integration, University of Stuttgart, Stuttgart, and is also the Head of the Institute for Micro Assembly Technology, Hahn-Schickard, Stuttgart.

...